Biochars from wood biomass as effective methylene blue adsorbents

Barbara Charmas [1], Barbara Wawrzaszek [1], Katarzyna Jedynak [2]

[1] Institute of Chemical Sciences, Faculty of Chemistry, Maria Curie-Sklodowska University, Maria Curie-Sklodowska Sq. 3, 20-031 Lublin, Poland

[2] Institute of Chemistry, Jan Kochanowski University, Uniwersytecka Str. 7, 25-406 Kielce, Poland

Corresponding author: barbara.charmas@mail.umcs.pl (Barbara Charmas)

Abstract: Forest waste is a significant ecological and economic problem, requiring effective solutions that will not only reduce its quantity but also contribute to the protection of the natural environment. This research paper focuses on the use of sawdust from mixed trees, as one of the main forest wastes, for production of biochars characterized by adsorption properties. Sawdust, a by-product of the wood industry, has a porous structure, which makes it an attractive precursor to biochar. Using pyrolysis technology and hydrothermal activation under various conditions, sawdust was transformed into biochars with a developed specific surface area. The studies proved that the parameters of the pyrolysis process have a significant impact on the structural, surface and adsorption properties of biochars. The materials were characterized based on the results of N_2 adsorption, scanning electron microscopy SEM/EDS, thermogravimetric analysis (TGA), Fourier Transform Infrared Spectroscopy (ATR-FTIR) and Raman spectroscopy. The surface characterization was made using the Boehm titration and pH_{pzc} determination. The sorption capacity of methylene blue (MB) was studied. It was stated, that the obtained materials were characterized by a large specific surface area (227.5 – 1019 m^2/g), the micro/mesoporous structure and the large pores volume (0.106 – 0.784 cm^3/g). The surface oxygen functionalities allowed for large adsorption of MB. The adsorption process follows the Langmuir theory ($q_{m,cal}$ from 357.1 to 434.8 mg/g) and can be described using the kinetic pseudo-second-order model (R^2 = 0.99). The obtained biochars showed high adsorption capacity of methylene blue impurities which indicates their significant potential for use in water purification.

Keywords: activated biochars, pyrolysis, hydrothermal activation, dye adsorption

1. Introduction

The intensive increase in environmental pollution observed in recent years and the need to search for alternative energy sources encourage researchers to look for innovative solutions in the field of waste management, including biomass. The reason is the slow depletion of fossil fuel resources: hard coal, lignite, oil and natural gas. It is predicted that the prices of these raw materials on the world market will continue to rise, which without the use of new technologies can lead to crises. Another reason for the interest in biomass is the increasingly widespread use of renewable energy sources. Biomass, by definition, is treated as a low-emission carrier in relation to carbon dioxide (CO_2). During photosynthesis, plants incorporate into their structures the same amount of carbon dioxide as they release during the combustion process, so they maintain the CO_2 balance in the atmosphere at zero (Saletnik et al., 2019).

Wood is a natural resource with specific physical and chemical properties useful in a wide range of applications, for example in construction, furniture, packaging or energy (Parham and Gray, 1984). Wood waste, including the forest waste (wood, branches, bark and sawdust), accounts for a significant proportion of wood industry waste. However, the plant biomass is quite difficult to use as a fuel and requires proper treatment because this is a heterogeneous, contaminated material, often damp and with a low energy potential (Saletnik et al., 2022). Traditionally, wood biomass was used as a fuel in energy processes, however, through innovative approaches, wood waste can be turned into a valuable

resource, not only reducing waste, but also producing biochar, a greatly efficient material with adsorption properties, commonly used for the environmental management applications that include soil remediation (Ding et al., 2016; Bianco et al., 2021), carbon sequestration (Lal, 2004; Woolf et al., 2010; Tenenbaum, 2013) or adsorption of heavy metals and other impurities, and many others (Kookana, 2010; Mohan et al., 2014; Liang et al., 2006; Chen and Pilla, 2022; Jedynak and Charmas, 2021; Wiśniewska et al., 2022; Szczęśniak et al., 2020; Skubiszewska-Zięba et al., 2017; Gusiatin et al., 2023). However, it should be remembered that wood biomass, being an available and cheap source of carbon in the form of organic compounds, is characterized by a very diverse structure. This is due to the structure of different tree species, processing methods, geographical conditions and even the season. However, the results of extensive research carried out around the world show that even if there is no exact reproducibility of the parameters of the starting materials, the use of wood biomass for the biochars production is a very beneficial solution and opens up new perspectives. The treatment of this waste to obtain biochar can contribute to the sustainable use of forest resources and the reduction of greenhouse gas emissions (Jeyasubramanian et al., 2021).

One promising biomass processing technology is pyrolysis, the process of thermal conversion of biomass to obtain biochar. Pyrolysis is a process in which biomass is subjected to a high temperature under the anaerobic conditions, leading to its chemical structure transformation into various products: biogas, bio-oil or biochar. Biochar is a porous carbon material with a developed surface area and rich surface chemistry, which makes it an excellent adsorption material, it has the ability to capture and retain pollutants, chemicals and heavy metals from various environments such as water, air or soil. The structure and surface characteristics of the resulting biochars depend on the structure of the starting material and the pyrolysis/activation conditions (Hindi, 2012; Zielińska et al., 2015; Jedynak and Charmas, 2021; Wiśniewska et al., 2022; Skubiszewska-Zięba et al., 2017).

Methylene blue (MB) is one of the common cationic dyes that is toxic, carcinogenic and mutagenic, and above all, persistent in the environment (Mishra et al., 2010). It is widely used in the industry for dyeing paper, leather, clothing and textile fabrics. The wide scale of industrial applications of this dye means that it is discharged together with sewage into soil and surface waters (Oladoye et al., 2022). MB can cause permanent damage to the eyes and skin, as well as have some negative effects on living beings, such as: delirium, excessive sweating when inhaled through water, irritation of the mouth, throat and stomach with the symptoms of nausea as well as diarrhea and vomiting (Jedynak et al., 2021). In large doses it can cause lethal serotonin toxicity to humans and also pose a threat to fauna in the aquatic ecosystem. Thus, it is very important to eliminate the MB dye from wastewater (Oladoye et al., 2022; Khan et al., 2022). One of the most effective treatment methods currently used is the use of activated carbons as adsorbents to remove dyes from wastewater (Wolski et al., 2023). Therefore, the aim of this paper was to analyze the potential of using sawdust from mixed trees for the production of biochars as well as the impact of various hydrothermal modification methods on structural, thermal, surface and adsorption characteristics in relation to methylene blue as a model pollutant. It is expected that the presented results of our research will provide new knowledge about the potential of using biochars obtained from forest waste and sawdust and will contribute to the development of sustainable methods of producing adsorption materials.

2.   Materials and methods

2.1. Materials

Sawdust of mixed trees came from the household. A large batch of material was collected at one time to avoid excessive variation in the composition of sawdust, e.g. due to heavy rainfall or a different season of waste collection. The chemical reagents (HCl, NaOH, $NaHCO_3$, Na_2CO_3, methylene blue) were purchased from Standard (Poland).

2.2. Materials preparation

Sawdust was rinsed with distilled water and dried (24h, 105 °C). The dried material was ground and fractionated, a fraction in the range of 1 - 2 mm was used for testing. The biomass pyrolysis was conducted in an inert gas atmosphere (N_2, gas flow 100 cm^3/min) by heating the system to 800 °C

(heating at 10 °C/min) and then maintaining the temperature of 800 °C for 1 hour. The resulting biochar was designated BC-800. Due to the poor development of the biochar surface, there were used additional different methods of hydrothermal activation: direct activation with the superheated steam during pyrolysis (method 1) and activation with water vapor using the microwave radiation as an energy source (method 2). During the pyrolysis combined with the superheated steam activation (method 1), the material was subjected to the oxidizing steam treatment in the heating stage at 800 °C (1h, water flow 0.6 cm^3/min). The resulting biochar was designated BC-800$_{H2O}$. Activation with water vapor using the microwave radiation as an energy source was performed in the microwave reactor "NANO 2000" (Plazmatronika, Wrocław, Poland) for 60 minutes in the pressure range of 77 - 80 atm. at 100% reactor power. The about 3g samples were placed in a quartz vessel and then in a Teflon tube of the reactor. The modifying factor was redistilled water (V = 25 cm^3) placed directly in the Teflon thimble. BC-800 and BC-800$_{H2O}$ biochars were activated and the modified materials were designated BC-800$_{MW}$ and BC-800$_{H2O-MW}$.

2.3.   Methods

2.3.1. Low-temperature adsorption/desorption nitrogen

In order to characterize the biochars porous structure, the low-temperature adsorption/desorption of nitrogen at -196 °C was performed using the ASAP 2405 apparatus (Micromeritics, Norcross GA, USA). From the obtained data the specific surface area S_{BET}, sorption pores volume V_p at p/p_s ~ 0.99 and average pores radius ($R_{av} = 2V_p/S_{BET}$) were determined (Gregg and Sing, 1982). Using the desorption branch data the dV/dlogD=f(D) functions were determined by means of the BJH method (Barrett et al., 1951).

2.3.2. Thermogravimetric analysis

The thermal properties and the proximate analysis were studied using Derivatograph C (Paulik, Paulik and Erdey, MOM, Hungary). The samples (~30 mg) were placed in the ceramic crucibles using aluminum oxide as the reference substance. The measurements were made in the temperature range of 20-1200 °C (10 °C/min, air atmosphere). The TG, DTG, and DTA curves were recorded. Additionally, the thermal analysis was performed in the nitrogen (temperature range 20 – 900 °C; 10 °C/min) to perform the proximate analysis of the materials. Based on the TGA data (N_2; 150 – 900 °C) the content of volatile matter (VM%) was determined. The ash content (A%) was calculated as the residue after the sample total oxidation (air; 1200 °C). The fixed carbon content (FC%) was estimated as the difference between the dry sample mass and ash as well as the volatile matter contents.

2.3.3. Raman spectroscopy

In order to obtain information about biochar matter structure there were made Raman spectra using inVia Reflex (Microscope DMLM Leica Research Grade, Reflex, Renishaw, UK). Excitation was achieved using the argon laser 785 nm.

2.3.4. SEM/EDS

In order to study the morphology of the biochars, the Quanta 3D FEG scanning electron microscope (FEI) was used. The measurements were performed under the low vacuum conditions at the voltage of 5 kV. The energy dispersive X-ray spectroscopy (SEM/EDS, acceleration: 20 kV) was used for quantitative and qualitative analyses.

2.3.5. ATR-FTIR

The infrared spectra were recorded using the Perkin-Elmer Spectrum 400-FT-IR/FT-NIR (Perkin-Elmer, Waltham, MA, USA) with the single diamond reflection and attenuated total reflection (ATR) endurance cell. Spectra in the range of 4000 - 650 cm^{-1} with a resolution of 4 cm^{-1} were recorded. The samples were dried and powdered before testing.

2.5.6. Potentiometric titration

The content of oxygen functional groups on the surface of carbon materials was determined by the Boehm potentiometric titration (Boehm, 2002). The samples (~0.2g) were filled with 10 cm³ portions of NaOH, HCl, NaHCO$_3$ (0.05 mol/L) or Na$_2$CO$_3$ (0.025 mol/L) solutions. After the neutralization process (24h), the concentrations of the solutions were tested using the potentiometric titrator (Titrino, Metrohm).

2.5.7. Zero charge point of biochar (pH$_{pzc}$)

The zero charge point (pH$_{pzc}$) was determined using the drift method (Rivera-Utrilla et al., 2001). The NaCl solution with the concentration of 0.01 mol/L was brought to pH in the range of 3 - 12 using the NaOH solutions with the concentrations of 0.1, 1 and 2 mol/L and the HCl solutions with the concentrations of 0.1 and 1 mol/L. The biochar samples (~ 0.1g) were poured with solutions of different pH values and placed in the shaker at 25 °C (100 rpm.) for 4 hours. After this time, the pH of the supernatant was measured. The relationship pH$_{final}$=f(pH$_{initial}$) was plotted. The intersection of the determined curve with the line pH$_{initial}$ = pH$_{final}$ determines the pH$_{pzc}$ point (Faria et al., 2004).

2.5.8.   Adsorption studies of methylene blue

2.5.8.1. MB adsorption kinetics

The batch method was applied for the methylene blue adsorption investigations. The research was carried out at 298K, 308K and 315K. The MB solutions (C$_0$ = 600 mg/L; V = 0.025 L) were added to the flasks containing activated carbons (0.05 g). The initial MB concentration was experimentally selected with 600 mg/L because at lower concentrations complete or nearly complete adsorption of the dye occurred. Therefore, this concentration was selected as optimal. The flasks were placed on the shaker (140 rpm; 24 hours). MB concentration was tested every 30 minutes (for 2 hours), then every 60 minutes (for 4 hours), every 120 minutes (3 measurements) and after 24 hours. The MB concentration measurements were made spectrophotometrically at the wavelength of 664 nm ("Helios Gamma", Spectro-Lab, Poland). The kinetics of the adsorption process was described on the basis of the linear equations of PFO (Eq. 1), PSO (Eq. 2) and Weber-Morris intra-particle diffusion model (Eq. 3) (Shafiq et al., 2021).

$$\ln(q_e - q_t) = \ln q_e - k_1 t \tag{1}$$

$$t/q_t = 1/(k_2 q_e^2) + t/q_e \tag{2}$$

$$q_t = k_{id} t^{1/2} + C \tag{3}$$

where: q$_t$ – the amount of adsorbed substance per 1 gram of adsorbent after time t [mg g^{-1}]; q$_e$ – the amount of adsorbed dye per 1 gram of adsorbent at equilibrium [mg g^{-1}]; k$_1$ - the reaction rate constant [min^{-1}]; k$_2$ - the reaction rate constant [g mg^{-1} min^{-1}]; k$_{id}$ – the intraparticle diffusion rate constant [mg g^{-1} min$^{1/2}$]; C –the boundary layer thickness [mg g^{-1}]; t – the adsorption time [min].

2.5.8.2. Determination of adsorption isotherms

Exact amounts of activated carbons (0.05 g) were placed in the Erlenmeyer flasks and the dye solutions (V = 0.025 L, the MB concentrations in the range 100 - 1500 mg/L) were added. The flasks were placed on a shaker (140 rpm; 24h). The tests were carried out at 298K, 308K, and 315K. The amount of adsorbed dye at equilibrium, q$_e$, was calculated from the following equation (Eq. 4):

$$q_e = ((C_0 - C_e) \cdot V)/m \tag{4}$$

where: q_e – the amount of adsorbed dye per 1 g of adsorbent at equilibrium [mg g^{-1}]; C$_0$ – the initial concentration of the dye solution [mg L^{-1}]; C$_e$ – the equilibrium concentration of the dye solution [mg L^{-1}]; V- the dye solution volume [L]; m – the sample mass [g].

To describe the adsorption isotherms the Langmuir (Eq. 5) and Freundlich (Eq. 6) linear models were used (Palanivell et al., 2020; Rigueto et al., 2020).

$$C_e/q_e = 1/q_m \times C_e + 1/q_m \times K_L \tag{5}$$

$$logq_e = logK_F + 1/n \, log \, C_e \qquad (6)$$

where: q_e – the amount of adsorbed substance per 1 gram of adsorbent in the equilibrium state [mg g^{-1}]; q_m – the maximum amount of adsorbed substance [mg g^{-1}]; C_e – the equilibrium concentration of the dye solution [mg L^{-1}]; K_L – the Langmuir adsorption equilibrium constant [L mg^{-1}]; K_F – the Freundlich constant which indicates the adsorption capacity [mg$^{1-1/n}$ (dm^3)$^{1/n}$ g^{-1}]; n - the Freundlich adsorption intensity constant.

There were also determined the functions describing the thermodynamics of the adsorption process: standard free energy change (ΔG), enthalpy change (ΔH) and entropy (ΔS) (Eqs. 7, 8).

$$\Delta G = -RTlnK_L \qquad (7)$$

$$lnK_L = -(\Delta H/R * 1/T) + \Delta S/R \qquad (8)$$

where: ΔG - standatd free energy change(kJ/mol); ΔH – enthalpy change (kJ/mol), ΔS - entropy (J/mol*K); R – the universal gas constant (8.314 J/mol*K); T – the absolute temperature (K); K_L – the equilibrium constant obtained from Langmuir model; drawing the van't Hoff plot of lnK_L versus $1/T$ allows to determine the ΔH and ΔS values from the slope and intercept.

3. Results and discussion

The crystal structure of biochars was characterized using Raman spectroscopy. In the examined materials there were distinguished two characteristic bands in the range of 1300 – 1600 cm^{-1}: the D and G bands (Fig. 1). The D band occurring at about 1350 cm^{-1} indicates the presence of sp^3 hybridized carbon structures in the hexagonal aromatic rings, while the G-band at about 1570 cm^{-1} is associated with the presence of sp^2 hybridized carbon atoms in the rings and chains of organic structures (Ferrari and Robertson, 2000; Li et al., 2017). It was found that with the use of activation, there is an increase in the intensity of the bands, which suggests an increase in the number of aromatic rings and a better ordering of carbon structures affected by the steam activation (Li et al., 2017). The ratio of intensity of the I_D/I_G bands allows to determine the dominant type of carbon structure of the material and the content of the disordered phase with sp^3 hybridization (Ferrari and Robertson, 2004). The determined intensity ratios of the I_D/I_G bands (in the range from 1.04 to 1.23, Fig. 1) indicate a significant number of defects in the structure of the studied biochars. With the use of additional activation, the I_D/I_G ratio increases slightly, indicating an increase in the order of the materials structure.
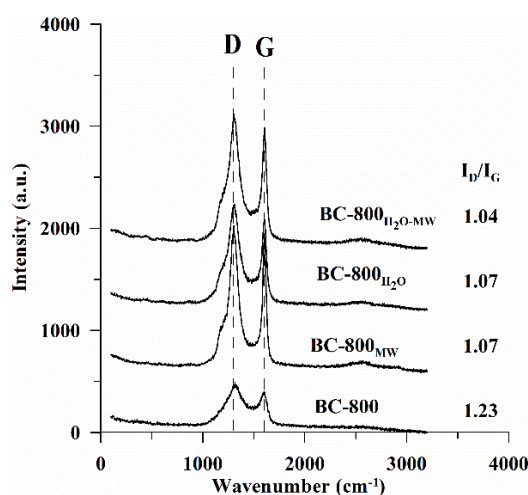
Fig. 1. Raman spectra of the nonactivated (BC-800) and activated biochars

Fig. 2a shows the low-temperature nitrogen adsorption/desorption isotherms determined for the material obtained by pyrolysis at 800 °C and activated biochars under various hydrothermal conditions. The shapes of the isotherms determined for BC-800 and BC-800$_{MW}$ belong to the type I isotherms and indicate a poorly developed surface area and the presence of only micropores in their structure. It can be observed that the steam modification using microwaves as a radiation source (BC-800$_{MW}$) caused

intensive development of the surface and structure of the micropores. This is evidenced by the location of the adsorption isotherm higher than the BC-800 biochar isotherm, especially in the area of low relative pressures at p/p_o up to 0.2 (Fig. 2a). According to the course of isotherms, steam modification in the pyrolysis stage was much more effective. The isotherms determined for the biochars BC-800$_{H2O}$ and BC-800$_{H2O-MW}$ belong to type IV, indicating the presence of micro- and mesopores in the biochar structure. The rising position of isotherms related to the relative pressure axis indicates increasing surface development and porosity. These materials are also characterized by a larger volume of micropores. The most effective is the modification of the biochar structure using two stages of steam activation. The pore volume distribution curves (Fig. 2b) confirm the effective development of the pore structure in the studied biochars under the influence of water vapor.
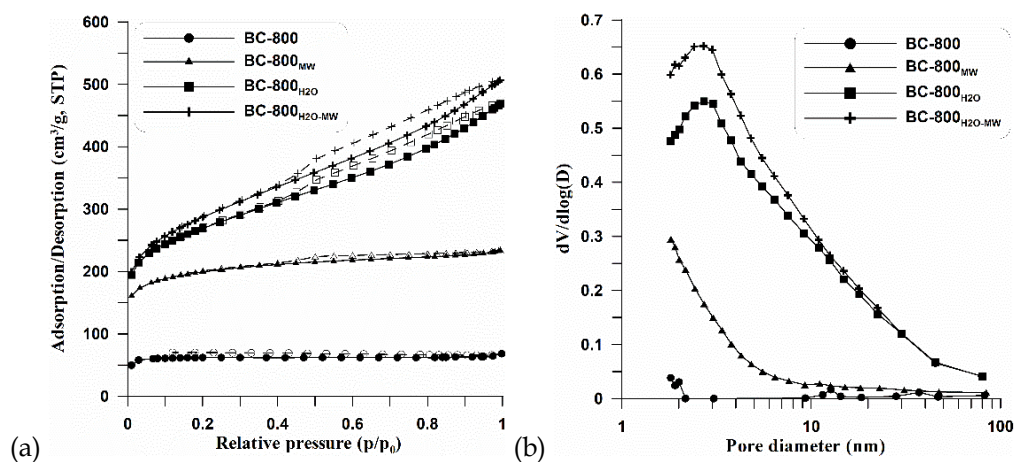
Fig. 2. Low temperature N_2 adsorption/desorption isotherms (a) and pore volume distribution curves (b) obtained for the tested biochars

Table 1 shows the structural parameters determined for the resulting biochars. The presented data indicate that the materials have a specific surface area ranging from 227.5 m²/g (BC-800) to 1019 m²/g (BC-800$_{H2O-MW}$). Intensive development of the porous structure and specific surface area of the obtained biochars was observed after the hydrothermal activation processes. The change in the specific surface area (S_{BET}, Table 1) after the application of microwave radiation is 501.7 m²/g, while after the modification with the superheated steam in the pyrolysis stage it is as much as 727.8 m²/g. Such a change indicates a much better efficiency of activation with the superheated steam under these conditions. The biochar BC-800$_{H2O-MW}$ is characterized by the largest specific surface area (1019 m²/g). As a result of the modification, the micropore area (S_{mi}) increased by about twice, however, the share of %S_{mi} in relation to the total S_{BET} area was significantly reduced (from ~90% for BC-800 to ~35% for BC-800$_{H2O-MW}$, Table 1). Such changes were also observed during the analysis of V_{mi} and %V_{mi} values. This may be due to excessive carbon oxidation which caused the collapse of the thin walls between the micropores resulting in the pore widening and R_{av} growth. This is also indicated by the observed increase in the total pore volume V_p and the mean pore radius R_{av} (Fig. 2b, Table 1).

Table 1. Structural characteristics of the obtained biochars

Sample	S_{BET}	ΔS_{BET}	S_{mi}	%S_{mi}	V_p	ΔV_p	V_{mi}	%V_{mi}	R_{av}
BC-800	227.5		208.4	91.6	0.11		0.09	82.1	0.93
BC-800$_{MW}$	729.2	501.7	494.2	67.8	0.36	0.26	0.26	56.8	0.99
BC-800$_{H2O}$	955.3	727.8	411.2	43.0	0.73	0.62	0.18	24.6	1.52
BC-800$_{H2O-MW}$	1019.0	791.5	363.1	35.6	0.78	0.68	0.16	20.0	1.54

where: S_{BET} – the specific surface area (m²/g), ΔS_{BET} – the change in the specific surface area size in relation to the no-activated biochar (m²/g), S_{mi} – the specific surface area of the micropores (m²/g), %S_{mi} – the percentage of the specific surface area of the micropores, V_p – the total volume of sorption pores (cm³/g), ΔV_p – the change in the total volume of sorption pores in relation to the nonactivated biochar (cm³/g), V_{mi} – the volume of micropores (cm³/g), %V_{mi} – the percentage of micropore volume, R_{av} – the mean pore radius (nm)

Table 2 shows the contents of various oxygen functional groups on the surface of the obtained biochars. The presence of both functional groups of acid and basic character, with the predominance of basic ones, was demonstrated. The number of basic groups varies from 1.13 to 1.71 mmol/g. BC-800$_{H2O-MW}$ biochar is characterized by the largest content of alkaline functionalities (1.71 mmol/g), activated by steam both in the pyrolysis process and additionally using microwaves as an energy source. Among the acidic groups, these are mainly phenolic (0.27 – 0.46 mmol/g, Table 2) and carboxyl (0.22 – 0.39 mmol/g) ones. The results of the study also proved the presence of a small number of surface lactone acidic groups (0.05 – 0.14 mmol/g).

Table 2. Chemical nature of the surface of the obtained carbons

Sample	Basic (mmol/g)	Acidic (mmol/g)	Acidic functionalities		
			Carboxyl (mmol/g)	Phenol (mmol/g)	Lactone (mmol/g)
BC-800	1.13	0.66	0.30	0.31	0.05
BC-800$_{MW}$	1.63	0.60	0.22	0.27	0.11
BC-800$_{H2O}$	1.18	0.67	0.23	0.30	0.14
BC-800$_{H2O-MW}$	1.71	0.91	0.39	0.46	0.06

The basic functional groups present on the surface of biochars affect the surface charge value (pH$_{pzc}$). pH$_{pzc}$ is the pH value at which the resultant surface charge of the adsorbent is zero. In the solution with pH < pH$_{pzc}$, the carbon surface has a positive charge, while for pH > pH$_{pzc}$ it has a negative charge. Fig. 3 shows the relationship between the final pH and the initial pH for the biochars to be tested. pH$_{pzc}$ for all tested biochars was approx. 11, which indicates that the adsorbent surface has a positive charge. The surface charge determines the adsorption properties of the material in relation to the selected adsorbates. Taking into account the electrostatic adsorbent-adsorbate interactions, MB, as a cationic dye, should be strongly adsorbed on the negatively charged carbon surface when pH>pH$_{pzc}$. However, in the analyzed case, other interactions should be taken into account because MB adsorbs very well on the surface of the carbon being examined despite the positively charged surface. In fact, there are possible various types of interactionse: (1) between the surface chromophore groups (acidic: e.g. alcohol, carbonyl and phenolic or basic: e.g. ketone, pyrone) of biochar and the cationic group in the dye molecule; (2) through hydrogen binding between the surface -OH groups and the nitrogen atom of the dye; (3) due to the interactions of the complex dye molecule with the π-electron system of the basic planes of carbon (Dogan et al., 2009).

The SEM images of the tested materials (Fig. 4) indicate a heterogeneous structure of biochars. The surface of the materials is rough and evidenced by numerous recesses and crevices of various sizes. The obtained biochars are made of an interconnected skeleton of channels, which indicates a partial preservation in the biochars of the original, fibrous structure of the starting materials (Fig. 4a,b) (Ma et al., 2016). The images taken at higher magnifications (x5000, Fig. 4c-e) indicate that the use of

	pH$_{pzc}$
♦ BC-800	11.62
▲ BC-800$_{MW}$	10.38
□ BC-800$_{H_2O}$	11.87
● BC-800$_{H_2O-MW}$	11.47
— pH$_{Initial}$ = pH$_{Final}$	
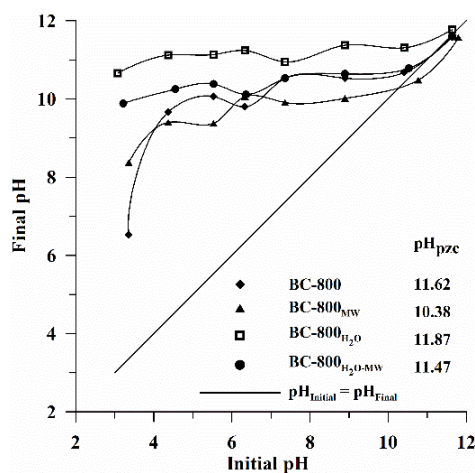
Fig. 3. Zero charge point (pH$_{pzc}$) of the tested biochars
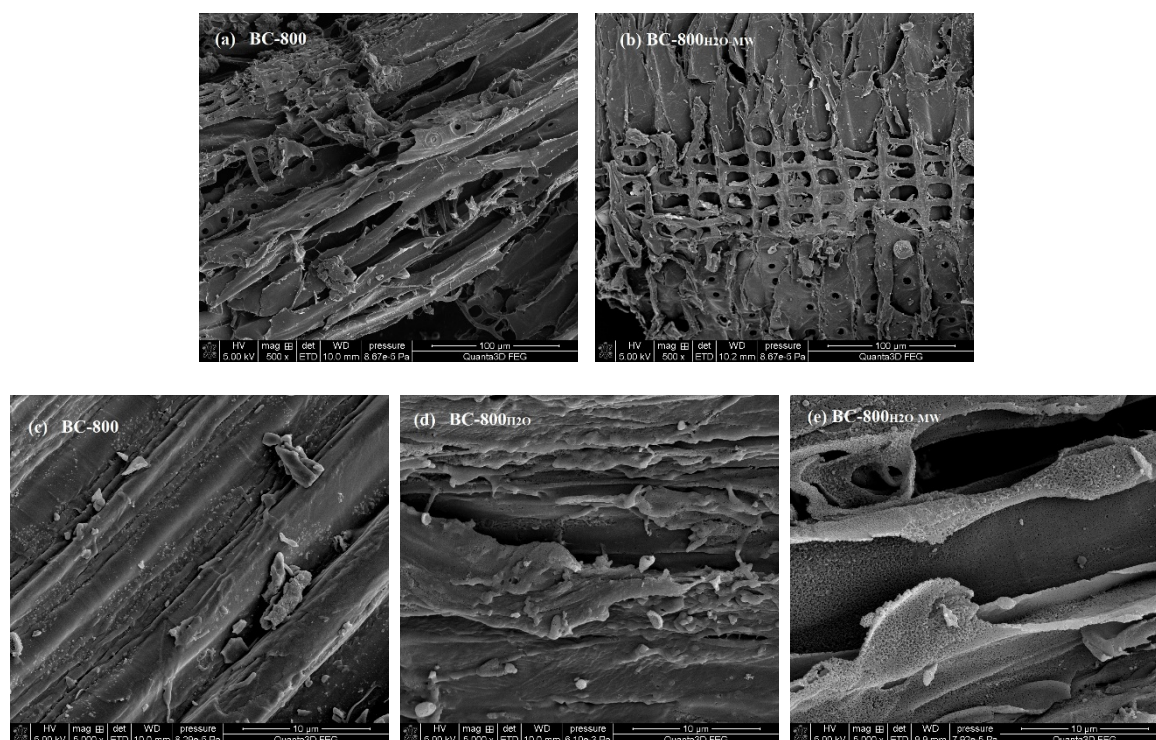
Fig. 4. SEM images of the biochars: BC-800 (a) and BC-800$_{H2O-MW}$ (b) mag. x500; as well as BC-800 (c), BC-800$_{H2O}$ (d) and BC-800$_{H2O-MW}$ (e) (mag. x5000)

hydrothermal modification results in the formation of a new structure of narrow pores, and the most effective pore formation was observed in the biochar BC-800$_{H2O-MW}$ (Fig. 4e).

The EDS analysis (Table 3) showed that biochars contain from 92.45% to 94.48% w/w carbon and from 4.08% to 5.03% w/w oxygen. The presence of these elements is associated with the presence of cellulose, lignin and hemicellulose in the initial sawdust (Mallakpour et al., 2021). The observed increase in the oxygen content may indicate the formation of surface oxygen groups during the activation. The biochars modified using the superheated steam in the pyrolysis stage are characterized by a slightly smaller carbon content (~ 1.5%, BC-800$_{H2O}$, BC-800$_{H2O-MW}$). In the case of the waste materials of organic origin, this is not a big difference, but it indicates clearly greater activation efficiency under these conditions compared to the steam activation using the microwave radiation as an energy source. Elements such as potassium, calcium, magnesium, silicon and sulfur are also present in biochars. Their occurrence is closely related to the chemical composition of the carbon precursor, and the variation in the content results from the heterogeneity of the waste precursor (Table 3).

Table 3. Elemental composition (%w/w) and proximate analysis (%) of the tested biochars

Sample	C	O	Na	Mg	Si	P	S	K	Ca	Mn	%VM	%FM	%A
BC-800	94.29	4.08	6.06	0.12	0.08	0.05	0.07	0.49	0.61	0.12	25.1	74.2	0.7
BC-800$_{MW}$	94.48	4.14	0.06	0.08	0.19	0.04	0.02	0.36	0.60	0.23	30.6	63.3	6.1
BC-800$_{H2O}$	92.87	4.81	0.09	0.19	0.26	0.10	0.02	1.06	0.54	0.06	20.9	77.8	1.3
BC-800$_{H2O-MW}$	92.45	5.03	0.09	0.13	0.37	0.05	0.05	1.02	0.69	0.08	18.1	75.2	6.7

The contents of carbon and inorganic components were also investigated using the thermal analysis (Table 3). The obtained biochars contain insignificant amounts of ash (0.7 – 6.7%, %A) and volatile matter (18.1 – 30.6%, %VM) as well as approx. 63 – 78% fixed mater (%FM).

The thermal analysis made it possible to assess the thermal stability of the biochars. The shape of the TG% curves (Fig. 5a) is similar for all tested samples. The curves indicate that the materials contained only a small amount of moisture and physically bound water, which is confirmed by a slight loss of mass and a poorly formed minimum on the DTG curve in the temperature range of 20 – 150 °C. At the

temperature of about 400 °C, there began thermal degradation, which occurred in two stages in all cases (Fig. 5b). The slope of the TG% curve varies in the temperature range of about 500 – 800 °C, which indicates a reduction of the thermal degradation rate due to the more durable fixed carbon (FC%) structure. This change is clearly visible on the DTG (Fig. 5b) and DTA (Fig. 5c) curves. A decrease in the width of DTG and DTA peaks was also observed (Fig. 5b,c), indicating a shorter degradation step time due to better arrangement of the biochar structure under the influence of hydrothermal activation.
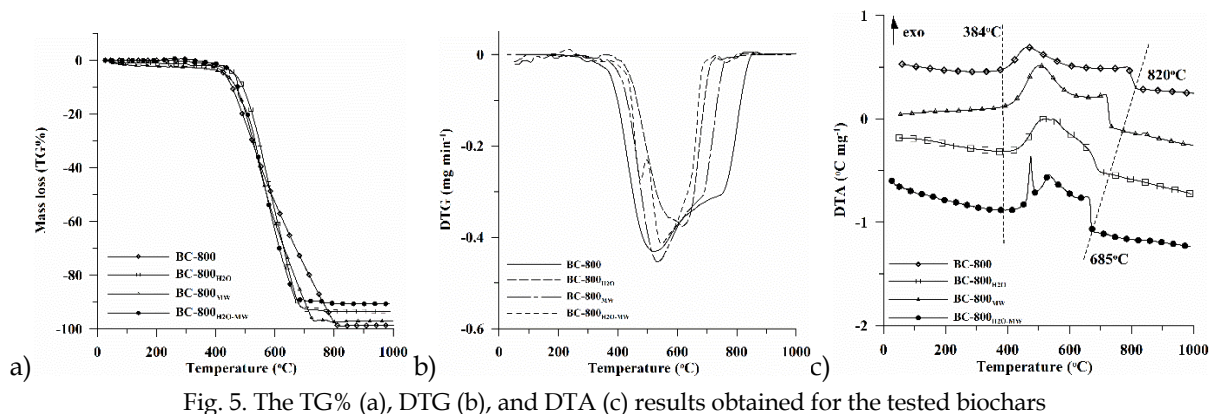
Fig. 5. The TG% (a), DTG (b), and DTA (c) results obtained for the tested biochars

As a result of the hydrothermal modification, aerobic functional groups were produced on the biochars surface. Such conclusions result from the EDS analysis and determination of the surface functional groups by potentiometric titration. This is also confirmed by the FTIR-ATR studies. The ATR-FTIR analysis (Fig. 6) revealed characteristic bands in the range of 3000 – 2800 cm^{-1} corresponding to the asymmetric tensile vibrations of the groups -CH$_2$, -CH$_3$ (Vaughn et al., 2013). Bands at 2164 cm^{-1} and 1979 cm^{-1} indicating the presence of the CO group were also observed (Ma et al., 2020). Their intensity increases after applying the steam modification in the pyrolysis stage (Fig. 6, BC-800$_{H2O}$, BC-800$_{H2O-MW}$). The bands at 1552 cm^{-1} and 1464 cm^{-1} originate from the C=O tensile vibrations of the carbonyl group, and their intensity also increased due to activation (Marciniak et al., 2018). The wide bandwidth at 1087 cm^{-1} and 1002 cm^{-1} corresponds to the tensile vibrations of the CO hydroxyl group (Ray et al., 2020). The 872 cm^{-1} band corresponds to the deformation C-H vibrations outside the plane in the aromatic rings occurring in the region of 900-750 cm^{-1} (Vaughn et al., 2013).
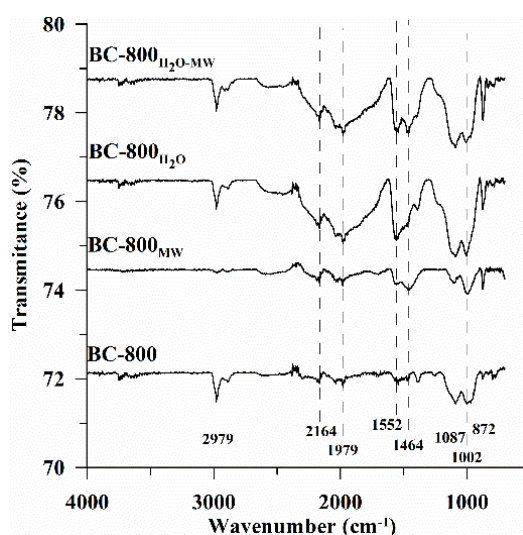
Fig. 6. The FTIR-ATR spectra obtained for the tested biochars

The BC-800$_{H2O}$ sample was selected for testing the possibility of using the biochar from the wood waste in the water purification processes due to its well-developed surface area (955.3 m^2/g) and pore volume (0.73 cm^3/g). Methylene blue (MB) was chosen as the model impurity. The preliminary MB adsorption studies examined the steady state settling time. It was proved that adsorption occurs very

intensively in the initial stage of the process. Equilibrium was most rapidly reached at 315K. The course of linear relationships resulting from the applied pseudo-first-order kinetic (Fig. 7a) and pseudo-second-order (Fig. 7b) models were determined, and Table 4 contains the appropriate kinetic parameters of the adsorption process. On the basis of the presented results, it was found that adsorption on the tested biochar is better described by the pseudo-second-order kinetic equation, which is confirmed by high values of correlation coefficients ($R^2 > 0.99$, Table 4).
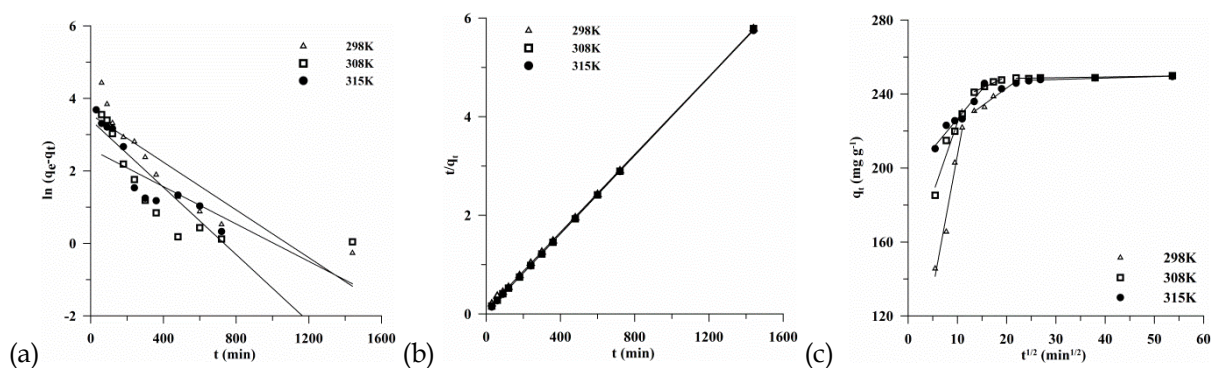
Fig. 7. Model of pseudo-first (a) and pseudo-second order (b) kinetics for BC-800$_{H2O}$ and the intra-particle diffusion model (c) at different temperatures

Table 4. Kinetics and intraparticle diffusion model parameters for the adsorption of methylene blue on BC-800$_{H2O}$

Temp.	Pseudo-first-order		Pseudo-second-order		Diffusion model		
[K]	k_1	R^2	k_2	R^2	k_{id}	C	R^2
298	0.0035	0.8065	0.0002	0.9998	14.481	62.108	0.9704
308	0.0029	0.6024	0.0005	0.9999	7.728	147.303	0.9200
315	0.0046	0.8434	0.0005	1	3.194	194.597	0.9569

where: k_1 - the reaction rate constant [min^{-1}]; k_2 - the reaction rate constant [g mg^{-1} min^{-1}]; k_{id} – the intraparticle diffusion rate constant [mg g^{-1} min$^{1/2}$]; C –the boundary layer thickness [mg g^{-1}]; R^2 – the correlation factor

The course of the adsorption process was also characterized using the intra-particle diffusion model (Fig. 7c). The course of the described relationships $q_t = f(t^{1/2})$ was adjusted using three (for the measurements made at 298K and 308K) or two (315K) linear segments, but in all cases the most intense changes in qt are observed in stage 1. The obtained graphs are used to explain the influence of intra-particle diffusion on the rate of the adsorption process. The diffusion process can be described by four steps (Sparks,1989):

1. transport of the adsorbate to the outer surface of the adsorbent;
2. diffusion through a layer of liquid surrounding the adsorbent particles to its outer surface;
3. diffusion of particles inside the pores and into the inner surface of the adsorbent;
4. adsorption and desorption in the particles and on the outer surface.

Diffusion inside the pores and on the inner surface of the adsorbent is described by the first section of the relationship ($q_t = f(t^{1/2})$, Fig. 7c). The determined diffusion rate constants (k_{id}) and the adsorption layer thickness (C) are shown in Table 4. The diffusion rate decreases with increasing temperature, which can be due to the exothermic nature of the adsorption process. The determined values of the parameter C take a positive value, which means that the intra-particle diffusion is not a step determining the speed of the entire adsorption process.

Fig. 8a shows the experimentally determined adsorption isotherms of methylene blue on biochar BC-800$_{H2O}$. The shape of the experimental isotherms indicates that adsorption occurs in the studied system according to the Langmuir theory. After high adsorption in the micropores, a plateau appears on the curves indicating the formation of a monolayer of dye molecules on the biochar surface. On the basis of the linear alignments of the adsorption isotherms of Langmuir (Eq. 5, Fig. 8b) and Freundlich (Eq. 6, Fig. 8c), the parameters of the corresponding equations were determined (Table 5). The analysis

of the data contained in Table 5 confirms that the adsorption process is better described by the Langmuir equation and the correlation coefficients are about $R^2 \sim 0.99$.
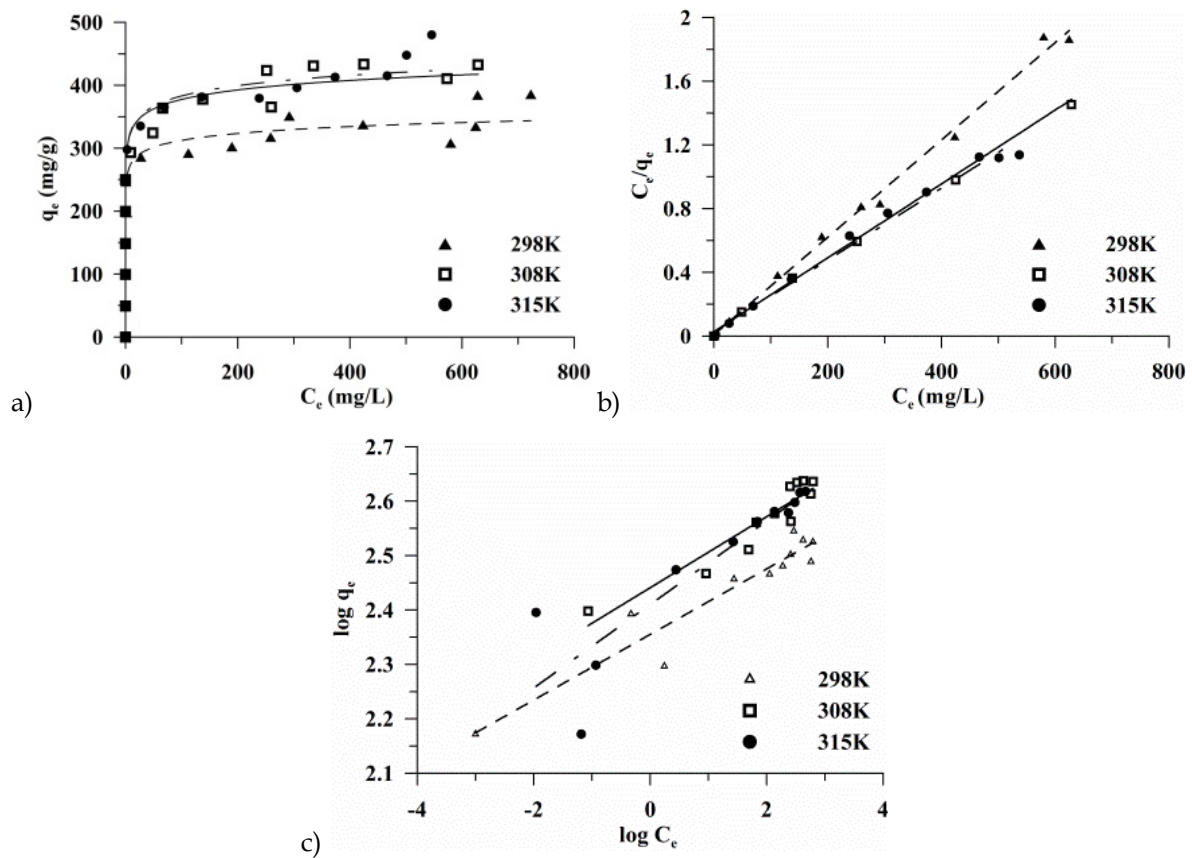
Fig. 8. Experimental MB adsorption isotherms (a) and linear fittings of isotherms according to the Langmuir (b) and Freundlich (c) models on BC-800$_{H2O}$ biochar

Table 5. Parameters of the Langmuir and Freundlich adsorption isotherm models

Model	Parameter	Temperature (K)		
		298	**308**	**315**
Langmuir	$q_{m,exp}$	385.7	433.5	479.9
	$q_{m,cal}$	357.1	434.8	434.8
	K_L	0.0067	0.0856	0.0920
	R^2	0.9813	0.9953	0.9907
Freundlich	K_f	227.8	275.9	258.2
	N	15.56	15.31	12.39
	R^2	0.8924	0.8797	0.8232

where: $q_{m,exp}$ – the amount of adsorbed substance per 1 gram of adsorbent in the equilibrium state (mg g^{-1}); $q_{m,cal}$ – the maximum amount of adsorbed substance (mg g^{-1}); K_L – the Langmuir adsorption equilibrium constant [L mg^{-1}]; K_F – the Freundlich constant which indicates the adsorption capacity [mg$^{1-1/n}$ L$^{1/n}$ g^{-1}]; N - the Freundlich adsorption intensity constant.

On the basis of the determined Langmuir adsorption equilibrium constants (K_L), there were calculated the functions describing the thermodynamics of the MB adsorption process on the tested biochar: the standard free energy change (ΔG), enthalpy change (ΔH) and entropy (ΔS), (Eqs. 7, 8). The negative values of ΔG = -24.93 kJ/mol (T = 298K), -25.54 kJ/mol (T = 308K) and -25.72 kJ/mol (T = 315K) indicate the spontaneous nature of the adsorption process ($\Delta G < 0$). A decrease in ΔG with the increasing temperature indicates an increase in the spontaneity of the process, which may be due to the fact that a

higher temperature is able to provide more energy to the adsorbate molecule and affect the adsorption process (Feng et al., 2015) Positive values of ΔH (15.01 kJ/mol) and ΔS (134.13 J/mol*K) point to the endothermic nature of the adsorption process and randomness at the solid/liquid interface during the adsorption process.

The obtained experimental data (Table 5) were compared with those available in the literature for other biochars (Table 6). It was shown that the tested biochar is characterized by good adsorption properties.

Table 6. Comparison of the maximum adsorption capacity MB of the prepared activated biochars with that of other carbon materials

Biochar	S_{BET} ($m^2 g^{-1}$)	Carbon precursor	activation	q_m ($mg\ g^{-1}$)	Ref.
BC-800$_{H2O}$	955.3	Sawdust	oxidizing steam treatment	385.7-479.9	This work
AC-2$_{3-CO2}$	720.9	Spent coffee grounds	H_3PO_4, N_2/CO_2	237.67	Charmas et al., 2023a
AC-1-OXMW	600.4	Wheat bran	CO_2 and steam, microwave radiation	212.59-241.95	Charmas et al., 2023b
P	964	Horsetail herb	K_2CO_3	334.4	Przytulska et al., 2022
BAC	1188	Banana peels	K_2CO_3	400	Nowicki et al., 2016
GAC	1198	Grapefruit peels	K_2CO_3	454.54	Nowicki et al., 2016
MAC	1077	Mandarin peels	K_2CO_3	357.14	Nowicki et al., 2016
PAC	836	Pomelo	K_2CO_3	208.33	Nowicki et al., 2016
Activated carbon	1083	Rattan sawdust	KOH	294.14	Hameed et al., 2007
PA7	616	Fermentation residues of corn stalks and leaves	CO_2	147	Wolski et al., 2023
AC$_K$	1052	fennel seeds	K_2CO_3	474	Paluch et al., 2023
ACZ1175	1757	Teak sawdust	$ZnCl_2$	614	Nguyen et al., 2019
ACK1075	1013	Teak sawdust	K_2CO_3	516	Nguyen et al., 2019
COSHTC3	876.14	Coconut shell	NaOH	200	Islam et al., 2013

4. Conclusions

This paper describes the process of pyrolysis of sawdust from the mixed trees and the influence of various conditions of the hydrothermal activation process on the properties of the obtained biochars. The efficiency of biochars in the adsorption process of methylene blue is also discussed. The studies proved that the parameters of the pyrolysis and activation process have a significant impact on the structural, surface and adsorption properties of biochars. The obtained biochars, depending on the activation method, are characterized by a micro/mesoporous structure and significant surface heterogeneity. As follows the use of superheated steam activation in the pyrolysis stage results in better surface development than the steam activation using microwave radiation as an energy source. On the biochars surface, there are numerous aerobic functionalities, especially of an acidic nature. The material showed a high adsorption capacity MB (q_m = 385.7 – 479.9 mg/g), which increases with the increasing temperature, indicating the endothermic nature of the process. This suggests a great potential for the use of biochar in water purification. The conclusions drawn from the research results can contribute to the development of sustainable methods of forest waste management, reducing waste and at the same time contributing to the protection of the aquatic environment. The use of sawdust for the production of adsorption biochars is a promising solution that combines ecological and economic aspects, contributing to sustainable development.

References

BARRETT, E.P., JOYNER, L.G., HALENDA, P.P. 1951. *The determination of pore volume and area distributions in porous substances. I. Computations from nitrogen isotherms.* J. Am. Chem. Soc. 73, 373-380.

BIANCO, F., RACE, M., PAPIRIO, S., OLESZCZUK, P., ESPOSITO, G., 2021. *The addition of biochar as a sustainable strategy for the remediation of PAH–contaminated sediments.* Chemosphere 263, 128274.

BOEHM, H.P., 2002. *Surface oxides on carbon and their analysis: a critical assessment.* Carbon 40(2), 145–149.

CHARMAS, B., ZIĘZIO, M., JEDYNAK, K., KUCIO, K., 2023a, *Quasi-isothermal (Q-TG), cryoporometric (DSC) and adsorption characterization of activated carbons.* J. Therm. Anal. Calorim. 148, 7403–7419.

CHARMAS, B., ZIĘZIO, M., JEDYNAK, K., 2023b. *Assessment of the porous structure and surface chemistry of activated biocarbons used for methylene blue adsorption.* Molecules 28, 4922.

CHEN, N., PILLA, S., 2022. *A comprehensive review on transforming lignocellulosic materials into biocarbon and its utilization for composites applications.* Composites Part C. 7, 100225.

DING, Y., LIU, Y., LIU, S., LI, Z., TAN, X., HUANG, X., ZENG, G., ZHOU, L., ZHENG, B., 2016. *Biochar to improve soil fertility. A review.* Agron. Sustain. Dev. 36, 36.

DOGAN, M., ABAK, H., ALKAN, M., 2009. *Adsorption of methylene blue onto hazelnut shell: Kinetics, mechanism and activation parameters.* J. Hazard. Mater. 164, 172.

FARIA, P.C.C., ÓRFAO, J.J.M., PEREIRA, M.F.R., 2004. *Adsorption of anionic and cationic dyes on activated carbons with different surface chemistries.* Water Res. 38(8), 2043-2052.

FENG, D., YU, H., DENG, H., LI, F., GE, C., 2015. *Adsorption Characteristics of Norfloxacin by Biochar Prepared by Cassava Dreg: Kinetics, Isotherms, and Thermodynamic Analysis.* BioResources 10(4), 6751-6768.

FERRARI, A., ROBERTSON, J., 2004. *Raman spectroscopy of amorphous, nanostructured, diamond-like carbon, and nanodiamond.* Phil. Trans. R. Soc. Lond. A. 362, 2477–2512.

FERRARI, A., ROBERTSON, J., 2000. *Interpretation of Raman spectra of disordered and amorphous carbon.* Phys. Rev. B 61(20), 14095–14107.

GREGG, S.J., SING, K.S.W., 1982. Adsorption, surface area and porosity. 2nd Edition, Academic Press, London.

GUSIATIN, M.Z., PASIECZNA-PATKOWSKA, S., BALINTOVA, M., KUŚMIERZ, M., 2023. *Treatment of wastewater from soil washing with soluble humic substances using biochars and activated carbon.* Energies 16(11), 4311.

HAMEED, B.H., AHMAD, A.L., LATIFF, K.N.A., 2007. *Adsorption of basic dye (methylene blue) onto activated carbon prepared from rattan sawdust.* Dyes Pigm. 75, 143-149.

HINDI, S.S.Z., 2012. *Contribution of parent wood to the final properties of the carbonaceous skeleton via pyrolysis.* Int. J. Sci. Eng. Invest. 1(8), 9-12.

ISLAM, M.A. AHMED, M.J., KHANDAY, W.A., ASIF, M., HAMEED, B.H., 2017. *Mesoporous activated coconut shell-derived hydrochar prepared via hydrothermal carbonization-NaOH activation for methylene blue adsorption.* J. Environ. Manage. 203, 237-244.

JEDYNAK, K., CHARMAS, B., 2021. *Preparation and characterization of physicochemical properties of spruce cone biochars activated by CO_2.* Materials 14, 3859.

JEDYNAK, K., REPELEWICZ, M., KURDZIEL, K., WIDEŁ, W., 2021. *Mesoporous carbons as adsorbents to removal of methyl orange (anionic dye) and methylene blue (cationic dye) from aqueous solutions.* Desalin. Water Treat. 220, 363–379

JEYASUBRAMANIAN, K., THANGAGIRI, B., SAKTHIVEL, A., DHAVEETHU, R.J., SEENIVASAN, S., VALLINAYAGAM, P., MADHAVAN, D., MALATHI, D.S., RATHIKA, B. 2021. *A complete review on biochar: Production, property, multifaceted applications, interaction mechanism and computational approach.* Fuel 292, 120243.

KHAN, I., SAEED, K., ZEKKER, I., ZHANG, B., HENDI, A. H., AHMAD, A., AHMAD, S., ZADA, N., AHMAD, H., SHAH, L. A., SHAH, T., & KHAN, I. 2022. *Review on Methylene Blue: Its Properties, Uses, Toxicity and Photodegradation.* Water, 14(2), 242.

KOOKANA, R.S., 2010. *The role of biochar in modifying the environmental fate, bioavailability, and efficacy of pesticides in soils: a review.* Aust. J. Soil Res. 48, 627-637.

Lal, R., 2004. *Soil carbon sequestration impacts on global climate change and food security.* Science 304, 1623-1627.

Li, M., Tang, Y., Ren, N., Zhang, Z. Cao, Y., 2017. *Effect of mineral constituents on temperature-dependent structural characterization of carbon fractions in sewage sludge-derived biochar.* J. Clean. Prod. 172, 3342-3350.

LIANG, B., LEHMANN, J., SOLOMON, D., KINYANGI, J., GROSSMAN, J., O'Neill, B., 2006. *Black carbon increases cation exchange capacity in soils.* Soil Sci. Soc. Am. J. 70, 1719-1730.

MA, R., MA, Y. GAO, Y. CAO, J., 2020. *Preparation of micro-mesoporous carbon from seawater-impregnated sawdust by low temperature one-step CO_2 activation for adsorption of oxytetracycline.* SN Appl. Sci. 2(2), 171.

MA, X., ZHOU, B., BUDAI, A., JENG, A., HAO, X., WEI, D., ZHANG, Y., RASSE, D., 2016. *Study of biochar properties by Scanning Electron Microscope – Energy Dispersive X-Ray Spectroscopy (SEM-EDX).* Commun. Soil Sci. Plant Anal., 47(5), 593-601.

MALLAKPOUR, S., SIROUS, F., HUSSAIN, C. M., 2021. *Sawdust, a versatile, inexpensive, readily available bio-waste: From mother earth to valuable materials for sustainable remediation technologies.* Adv. Colloid Interface Sci., 295, 102492.

MARCINIAK, M., GOSCIANSKA, J., PIETRZAK, R., 2018. *Physicochemical characterization of ordered mesoporous carbons functionalized by wet oxidation.* J. Mater. Sci. 53, 5997 – 6007.

MISHRA, A.K., AROCKIADOSS, T., RAMAPRABHU, S. 2010. *Study of removal of azo dye by functionalized multi-walled carbon nanotubes.* Chem. Eng. J, 162(3), 1026-1034.

MOHAN, D., SARSWAT, A., OK, Y.S., PITTMAN, C.U., 2014. *Organic and inorganic contaminants removal from water with biochar, a renewable, low cost and sustainable adsorbent - A critical review.* Bioresour. Technol. 160, 191-202.

NGUYEN, H.D., TRAN, H.N., CHAO, H.-P., LIN, C.-C., 2019. Activated carbons derived from teak sawdust-hydrochars for efficient removal of methylene blue, copper, and cadmium from aqueous solution, Water 11, 2581.

NOWICKI, P., KAZIMIERCZAK-RAZNA, J., PIETRZK, R., 2016. *Physicochemical and adsorption properties of carbonaceous sorbents prepared by activation of tropical fruit skins with potassium carbonate.* Mater. Design 90, 579–585

OLADOYE, P.O., AJIBOYE, T.O., OMOTOLA, E.O., OYEWOLA, O.J., 2022. Methylene blue dye: Toxicity and potential elimination technology from wastewater. Results Eng. 16, 100678.

PALANIVELL, P., AHMED, O.H., LATIFAH, O., MAJID, N.M.A., 2020. *Adsorption and desorption of nitrogen, phosphorus, potassium, and soil buffering capacity following application of chicken litter biochar to an acid soil.* Appl. Sci. 10, 295.

PALUCH, D., BAZAN-WOZNIAK, R., PIETRZAK, R., 2023. *The effect of activator type on physicochemical and sorption properties of nanostructured carbon adsorbents obtained from fennel seed by chemical activation.* Appl. Nanosci. https://doi.org/10.1007/s13204-023-02890-7.

PARHAM, R., GRAY, A., 1984. *The chemistry of solid wood. Chapter 1: Formation and structure of wood.* ACS, Washington DC.

PRZYTULSKA, A., GORBOL, M., GIL-KOWALCZYK, M., NOWICKI, P., 2022. *Removal of methylene blue from aqueous solutions via adsorption on activated biocarbon obtained from post-extraction residue.* Physicochem. Probl. Miner. Process. 58(2), 146357.

RAY, A., BANERJEE, A., DUBEY, A. 2020. *Characterization of Biochars from Various Agricultural By-Products Using FTIR Spectroscopy, SEM focused with image Processing.* Int. J. Agric. Environ. Biotechnol. 13(4), 423-430.

RIGUETO, C.V.T., PICCIN, J.S., DETTMER, A., ROSSETO, M., DOTTO, G.L., De OLIVEIRA SCHMITZ, A.P., PERONDI, D., MARTINS De FREITAS, T.S., LOSS, R.A., GERALDI, C.A.Q., 2020. *Water hyacinth (Eichhornia crassipes) roots, an amazon natural waste, as an alternative biosorbent to uptake a reactive textile dye from aqueous solutions.* Ecol. Eng. 150, 105817.

RIVERA-UTRILLA, J., BAUTISTA-TOLEDO, I., FERRO-GARCIA, M.A., MORENO-CASTILLA, C., 2001. *Activated carbon surface modifications by adsorption of bacteria and their effect on aqueous lead adsorption.* J. Chem. Technol. Biotechnol. 76(12), 1209–1215.

SALETNIK, B., SALETNIK, A., ZAGUŁA, G., BAJCAR, M., PUCHALSKI, C., 2022. *The Use of Wood Pellets in the Production of High Quality Biocarbon Materials.* Materials, 15, 4404.

SALETNIK, B., ZAGUŁA, G.; BAJCAR, M., TARAPATSKYY, M., BOBULA, G., Puchalski, C., 2019. *Biochar as a Multifunctional Component of the Environment. Review.* Appl. Sci. 9, 1139.

SHAFIQ, M., ALAZBA, A.A., AMIN, M.T., 2021. *Kinetic and isotherm studies of Ni^{2+} and Pb^{2+} adsorption from synthetic wastewater using Eucalyptus camdulensis - derived Biochar.* Sustainability. 13, 3785.

SKUBISZEWSKA-ZIĘBA, J., CHARMAS, B., KOŁTOWSKI, M., OLESZCZUK, P., 2017. *Active carbons from waste biochars. Structural and thermal properties.* J. Therm. Anal. Calorim. 130, 15–24.

SPARKS, D.L., 1989. *Kinetics of Soil Chemical Processes.* Academic Press, New York, 1989.

SZCZEŚNIAK, B., PHURIRAGPITIKHON, J., CHOMA, J., JARONIEC, M., 2020. *Recent advances in the development and applications of biomass-derived carbons with uniform porosity.* J. Mater. Chem. A. 36, 18464-18491.

TENENBAUM, T.N., 2013. *Biochar: carbon mitigation from the ground up*. Sustain. Soil Manag., 117, 31-36.

VAUGHN, S.F., KENAR, J.A., THOMPSON, A.R., PETERSON, S.C., 2013. *Comparison of biochars derived from wood pellets and pelletized wheat straw as replacements for peat in potting substrates.* Ind Crops Prod . 51, 437–443.

WIŚNIEWSKA, M., REJER, K., PIETRZAK, R., NOWICKI, P., 2022. *Biochars and activated biocarbons prepared via conventional pyrolysis and chemical or physical activation of mugwort herb as potential adsorbents and renewable fuels*. Molecules. 27, 8597.

WOLSKI, R., BAZAN-WOZNIAK, A., PIETRZAK, R., 2023. *Adsorption of methyl red and methylene blue on carbon bioadsorbents obtained from biogas plant waste materials*, Molecules 28, 6712.

WOOLF, D., AMONETTE, J.E., STREET-PERROTT, F.A., LEHMANN, J., Joseph, S., 2020. *Sustainable biochar to mitigate global climate change*. Nat. Commun. 1, 56.

ZIELIŃSKA, A., OLESZCZUK, P., CHARMAS, B., SKUBISZEWSKA-ZIĘBA, J., PASIECZNA-PATKOWSKA, S., 2015. *Effect of sewage sludge properties on the biochar characteristic.* J. Anal. Appl. Pyrol. 112, 201-213.